Toxicology Letters 225 (2014) 57–65

Contents lists available at ScienceDirect

Toxicology Letters

journal homepage: www.elsevier.com/locate/toxlet

Interaction of polyacrylic acid coated and non-coated iron oxide nanoparticles with human neutrophils

Diana Couto[a], Marisa Freitas[a], Vânia Vilas-Boas[b], Irene Dias[a], Graça Porto[c], M. Arturo Lopez-Quintela[d], José Rivas[e], Paulo Freitas[e], Félix Carvalho[b], Eduarda Fernandes[a,*]

[a] REQUIMTE, Laboratory of Applied Chemistry, Department of Chemical Sciences, Faculty of Pharmacy, University of Porto, Porto, Portugal
[b] REQUIMTE, Laboratory of Toxicology, Department of Biological Sciences, Faculty of Pharmacy, University of Porto, Porto, Portugal
[c] Service of Clinical Hematology, Santo António Hospital, Porto, Portugal
[d] Laboratory of Nanotechnology and Magnetism, Institute of Technological Research, IIT, University of Santiago de Compostela (USC), Santiago de Compostela, Spain
[e] International Iberian Nanotechnology Laboratory, Braga, Portugal

HIGHLIGHTS

- Polyacrylic acid-coated iron oxide nanoparticles increase neutrophils' apoptosis.
- Non-coated iron oxide nanoparticles prevent neutrophils' apoptosis.
- Both nanoparticles trigger neutrophils' oxidative burst by NADPH oxidase activation.

ARTICLE INFO

Article history:
Received 30 August 2013
Received in revised form
17 November 2013
Accepted 18 November 2013
Available online 26 November 2013

Keywords:
Nanotoxicology
Oxidative burst
Apoptosis
Human neutrophils
Iron oxide nanoparticles
Polyacrylic acid coating

ABSTRACT

Iron oxide nanoparticles (ION), with different coatings and sizes, have attracted extensive interest in the last years to be applied in drug delivery, cancer therapy and as contrast agents in imagiologic techniques such as magnetic resonance imaging. However, the safety of these nanoparticles is still not completely established, particularly to host defense systems that are usually recruited for their clearance from the body. In this paper, given the importance of neutrophils in the immune response of the organism to nanoparticles, the effect of polyacrylic acid (PAA)-coated and non-coated ION on human neutrophils was evaluated *in vitro*, namely their capacity to activate the oxidative burst and to modify their lifespan. The obtained results showed that the studied PAA-coated and non-coated ION triggered neutrophils' oxidative burst in a NADPH oxidase dependent manner, and that PAA-coated ION increased — while non-coated ION prevented — apoptotic signaling and apoptosis. These effects may have important clinical implications in biomedical applications of ION.

1. Introduction

Nanotechnology is nowadays at the forefront in the development of new therapeutic and diagnostic tools in all areas of medicine (Shubayev et al., 2009). A good example of nanotechnology applications is brought by the use of iron oxide nanoparticles (ION), due to their multifunctional properties, conferred by their small size, superparamagnetism, and biocompatibility (Mou et al., 2011). In fact, ION have the potential to be extensively used for the improvement of site-specific drug delivery to cells, tissues, or even organs, as well as in the enhancement of magnetic resonance imaging contrast, hyperthermia treatments in cancer therapy, magnetofection, stem cell therapy and gene delivery (Hong et al., 2011; Muller et al., 2007; Naqvi et al., 2010; Shubayev et al., 2009). To prevent the precipitation of iron oxide cores, ION for medical imaging are always coated with a layer of protective and biocompatible colloid, usually a polymer that acts as a steric and/or electrostatic stabilizer (Roohi et al., 2012). In particular, the polyacrylic acid (PAA) coating is an aqueous soluble polymer with a high density of reactive functional groups that make it very attractive in biomedicine, mainly due to its capability to form flexible polymer chain-protein complexes trough electrostatic, hydrogen bonding or hydrophobic interactions (Pineiro-Redondo et al., 2011).

* Corresponding author. Tel.: +351 220428675.
E-mail address: egracas@ff.up.pt (E. Fernandes).

0378-4274/$ – see front matter © 2013 Elsevier Ireland Ltd. All rights reserved.
http://dx.doi.org/10.1016/j.toxlet.2013.11.020

Surface coating and size affect biodistribution, plasma half-life, and extent of cellular uptake of nanoparticles (Muller et al., 2007; Roohi et al., 2012). *In vivo*, large ION (comprised between 60 and 100 nm) are rapidly phagocytosed by cells of the reticuloendothelial system in the liver and spleen, having thereby a short blood half-life. On the other hand, small ION (<60 nm) are not readily phagocytosed, which results in a longer plasma half-life and higher availability to other cells and organs of the immune system (Matsushita et al., 2011; Muller et al., 2007). Although ION may represent extremely useful tools in biomedicine, there are still few studies assessing their possible effects in the above mentioned host defense systems that are usually recruited for their clearance from the body. It was previously reported that ION have the ability to decrease the monocytes' viability (Zhu et al., 2011), as well as to induce the production of reactive oxygen species (ROS) on macrophages and decrease their viability, through apoptosis, in a concentration-dependent manner (Lunov et al., 2010a,b; Naqvi et al., 2010). However, the effect of ION on neutrophils is still to be clarified, this being the purpose of the present study.

Human neutrophils are the most abundant leukocytes in blood and constitute the first line of innate host defense against pathogens and associated acute inflammations (Bockmann et al., 2001; Fadeel et al., 1998; Freitas et al., 2008). Neutrophils are mobilized to the sites of invasion or inflammation, ingesting pathogens into phagosomes (Fadeel et al., 1998; Freitas et al., 2009a,b, 2008). The phagosome fuses with neutrophilic cytoplasmatic granules containing cytotoxic enzymes, namely lysosomal enzymes, as well as NAPDH oxidase and myeloperoxidase, which are responsible for the oxidative burst and consequent generation of ROS (Brasen et al., 2010; Fadeel et al., 1998; Freitas et al., 2009a,b, 2008). While these events are important for the elimination of pathogens, it is not clear how these cells cope with ION, and which consequences ION have on their lifespan.

Neutrophils have a short lifespan that is regulated by the onset of apoptosis. In fact, apoptosis in mature neutrophils is a constitutive process that results in a rapid turnover of the circulating neutrophil population [(5×10^{10} neutrophils per day are released from bone marrow (Goncalves et al., 2010)] with a $t_{1/2}$ of 5 to 6 h *in vivo* and 24 to 36 h *in vitro* (Watson et al., 1998). This process is essential for the normal resolution of inflammation in tissues, because it culminates in the recognition and clearance of the apoptotic neutrophils by macrophages (Rowe et al., 2002). While it has been postulated that these cells undergo apoptosis spontaneously (Goncalves et al., 2010; Rowe et al., 2002), external factors may influence this process, as we have previously shown (Freitas et al., 2013a), and therefore the influence of the different nanoparticles in this process requires further investigation.

Necrosis is an unorganized process associated with extensive damage, resulting in an intense inflammatory response. In neutrophils, this process may occur due to a lack of intracellular adenosine triphosphate (ATP), necessary to apoptosis. Due to the energy-consumptive oxidative burst and consequent depletion of intracellular ATP stores, these cells may be unable to maintain cellular homeostasis and membrane integrity, occurring an influx of water and extracellular ions. This influx will trigger the intracellular organelles and the whole cell swelling, with all the cellular contents being released into the extracellular fluid and surrounding tissues (Kroemer et al., 2007; Turina et al., 2005).

Considering the lack of knowledge on the activation of neutrophils and modulation of their lifespan by ION, the aim of this work was to evaluate the effects of ION in magnetite form (polyacrylic acid (PAA)-coated and non-coated) on human neutrophils, namely their capacity to activate the oxidative burst and to modify their lifespan through necrosis and/or apoptosis.

2. Materials and methods

2.1. Materials

Human venous blood was obtained from healthy human volunteers from Hospital de Santo António (Porto, Portugal). Histopaque 1077, histopaque 1119, Dulbecco's phosphate buffer saline, without calcium chloride and magnesium chloride (PBS) [2.68 mM KCl, 0.14 M NaCl, 1.21 mM KH_2PO_4, 8.10 mM Na_2HPO_4], RPMI 1640 medium, L-glutamine, penicillin, streptomycin, trypan blue solution 0.4%, phorbol 12-myristate 3-acetate (PMA), dihydrorhodamine 123 (DHR), diphenyleneiodonium chloride (DPI), *N*-acetyl-Ile-Glu-Thr-Asp-*p*-nitroanilide, *N*-acetyl-Asp-Glu-Val-Asp-*p*-nitroanilide, Ac-Leu-Glu-His-Asp-*p*-nitroanilide, potassium phosphate, phenlymethylsulfonyl fluoride, leupeptin, pepstatin, HEPES and ethylenediamine tetraacetic acid (EDTA) were obtained from Sigma Chemical Co (St Louis, USA). β-Nicotinamide adenine dinucleotide reduced dipotassium salt (NADH), sodium pyruvate, CHAPS, triton™ X-100, dithiothreitol, ferrous chloride, ferric chloride, NH_4OH, KCl and polyacrylic acid PAA (average M_w 1800) were obtained from Sigma-Aldrich (St Louis, USA). Hemacolor® was obtained from Merck (Darmstadt, Germany). (±)-Nutlin-3 was acquired from Cayman (Michigan, USA). Sucrose was obtained from Mallinckrodt Chemical Works (St Louis, USA). Annexin-V-FLUOS Staining Kit was obtained from Roche Diagnostics GmbH (Mannheim, Germany). Nuclear Extract Kit and TransAM™ p53 Transcription Factor Assay Kits were acquired from Active Motif (La Hulpe, Belgium).

2.2. Methods

2.2.1. Synthesis of iron oxide nanoparticles

ION "non-coated" magnetite particles were prepared following previous well-known procedures with some modifications (Massart et al., 1995). In brief, the procedure is based on the chemical co-precipitation of a mixture of Fe(II) and Fe(III) chloride salts (molar ratio 2:1) using NH_4OH in a degassed 1 M KCl aqueous solution at 60 °C. The dark precipitate was washed several times with deoxygenated water, and finally the particles were stored at pH 9.6 (well-above their isoelectric point: 6.5). For the PAA-coated particles, PAA (25% w/w with respect to the Fe(II) salt) was added to the reaction medium.

2.2.2. Characterization of iron oxide nanoparticles

Non-coated and PAA-coated ION were characterized using transmission electron microscopy (TEM) (Hitachi H-7000, Japan). Determination of the hydrodynamic size and zeta potential of the nanoparticles in water suspensions, in function of pH and [NaCl], as well as in the medium used for the studies on human neutrophils [RPMI 1640 (pH = 7.4) supplemented with 10% fetal bovine serum, 2 mM L-glutamine, 100 U/mL penicillin and 0.1 mg/mL streptomycin] were made using a nanoparticle analyzer SZ-100 (HORIBA Scientific) (DPSS laser 532 nm). Before the dilutions, ION were sonicated for 5 min in order to avoid the formation of aggregates before the preparation of the samples.

2.2.3. Isolation of human neutrophils by the gradient density centrifugation method

Following informed consent, venous blood was collected from healthy human volunteers by antecubital venipuncture, into vacuum tubes with K_3EDTA. The isolation of human neutrophils was performed by the gradient density centrifugation method as previously reported in (Freitas et al., 2008). RPMI 1640 supplemented with 10% fetal bovine serum, 2 mM L-glutamine, 100 U/mL penicillin and 0.1 mg/mL streptomycin was the incubation medium used.

2.2.4. Measurement of neutrophils' oxidative burst

The measurement of neutrophils' oxidative burst was performed by fluorescence, by monitoring the oxidation of DHR to rhodamine 123 by neutrophil-generated reactive species (Freitas et al., 2009a,b). Neutrophils (3×10^6 mL^{-1}) were incubated for 24 h with PAA-coated and non-coated ION (4, 20 and 100 μg/mL) and DHR (10 μM) at 37 °C. At the end of this incubation period, cells were centrifuged (400*g*, 5 min at 20 °C) and the supernatant was discarded. The pellets were resuspended in 300 μL RPMI 1640 medium and the fluorescence was measured in a microplate reader ($\lambda_{excitation}$ = 485 nm and $\lambda_{emission}$ = 520 nm). PMA was used as positive control. Simultaneously it was performed an experiment where the neutrophils were incubated with ION (20 and 100 μg/mL), DPI (20 μM) and DHR (10 μM).

2.2.5. Evaluation of cellular necrosis

2.2.5.1. Trypan blue assay. Trypan blue assay was performed according to (Freitas et al., 2010). Neutrophils (2×10^6 mL^{-1}) were incubated with PAA-coated and non-coated ION (4, 20 and 100 μg/mL) for 24 h, at 37 °C. At the end of the incubation period, 20 μL aliquots of neutrophil suspensions were added to an equal volume of 0.4% trypan blue in a microtube and gently mixed. After 2 min on ice, the neutrophil number and viability (viable cells excluding trypan blue) were determined. This dye enters in the necrotic cells, staining them blue, while the living cells remain discoloured.

2.2.5.2. Lactate dehydrogenase (LDH) leakage assay. LDH leakage was performed according to (Freitas et al., 2010). This release is directly related to the cellular membrane disruption and, consequently, cellular death. Neutrophils (2×10^6 mL^{-1}) were incubated with PAA-coated and non-coated ION (4, 20 and 100 μg/mL) for 24 h at 37 °C. At the end of the incubation period, cells were centrifuged (6500*g*, 2 min at 4 °C) and the supernatant was collected. Simultaneously it was performed a control assay with sonicated cells in order to determine the total LDH. LDH activity was determined by following the rate of oxidation of NADH at 340 nm.

2.2.6. Evaluation of apoptosis

2.2.6.1. Evaluation of apoptosis by morphology. Evaluation of apoptosis by morphology was performed according to (Saldanha-Gama et al., 2010). Neutrophils (1×10^6 mL^{-1}) were incubated with PAA-coated and non-coated ION (4, 20 and 100 μg/mL) for 16 and 24 h at 37 °C. At the end of these incubation periods, cells were centrifuged in a microscopic slide (Cytospin, 300 rpm, 6 min at room temperature), stained with Hemacolor®, and counted under light microscopy to determine the proportion of cells showing characteristic apoptotic morphology (round and dark nucleus that results from the chromatin condensation occurring in apoptosis, signaled with arrows). At least 400 cells were counted per slide.

2.2.6.2. Evaluation of apoptosis by flow cytometry. Apoptotic neutrophils were analysed by flow cytometry after simultaneous staining with annexin-V labeled with fluorescein and propidium iodide, according to (Sladek et al., 2005). Annexin-V is a Ca^{2+}-phospholipid-binding protein that has a high affinity for phosphatidylserine and propidium iodide is impermeant to live cells and apoptotic cells, but stains dead cells with red fluorescence, tightly binding to the nucleic acids in the cell. The commercial Annexin-V-FLUOS Staining Kit (Roche Diagnostics GmbH, Mannheim Germany) was used according to the manufacturer's instructions. Neutrophils (1×10^6 mL^{-1}) were incubated with PAA-coated and non-coated ION (4, 20 and 100 μg/mL) for 16 h, at 37 °C. At the end of the incubation period, cells were centrifuged (400*g*, 5 min at 20 °C) and the supernatant was discarded. Pellets were resuspended in 1 mL of PBS and centrifuged (200*g*, 5 min at 20 °C). After centrifugation, pellets were resuspended in 100 μL of annexin-V and were incubated for 15 min in the dark. After incubation, samples were centrifuged (200*g*, 5 min at 20 °C) and the pellet was resuspended in 300 μL PBS and 3 μL propidium iodide.

Fluorescence signals for each sample were collected using a Becton Dickinson FACSCalibur™ flow cytometer (Becton Dickinson, Inc., Mountain View, CA, USA) equipped with a 488 nm argon-ion laser, as described in Freitas et al. (2013b).

2.2.7. Evaluation of pro-apoptotic signalling

2.2.7.1. p53-DNA binding. Neutrophils (8×10^6 mL^{-1}) were incubated with PAA-coated and non-coated ION (4, 20 and 100 μg/mL) for 24 h at 37 °C. At the end of this incubation period, neutrophils' desoxyribonucleic acid (DNA) was extracted using a Nuclear Extract Kit (Active Motif) according to manufacturer's instructions, with slight modifications. In order to obtain a more efficient nuclear extraction, sonication (4 cycles, 12 s) was performed to disrupt neutrophils' nuclear membrane before centrifugation (14,000*g*, 10 min 4 °C). Cell lysates were diluted to 3.5 μg total protein with lysis buffer and used for the p53 determination. For this purpose, TransAM™ p53 Transcription Factor Assay Kit was used according to manufacturer's instructions, as described in Thompson et al. (2004). (±)-Nutlin-3 was used as positive control.

2.2.7.2. Measurement of caspases 3, 8 and 9 activities. Neutrophils (10×10^6 mL^{-1}) were incubated with PAA-coated and non-coated ION (4, 20 and 100 μg/mL) for 16 and 24 h at 37 °C. At the end of these incubation periods, cells were centrifuged (400*g*, 5 min at 20 °C) and the supernatant was discarded. Pellets were resuspended in 100 μL of lysis buffer (10 mM potassium phosphate, 1 mM EDTA, 0.5% Triton X-100, 2 mM phenlymethylsulfonyl fluoride, 3 μg/mL aprotinin, 10 μg/mL leupeptin, 10 μg/mL pepstatin, and 10 mM dithiothreitol). After incubation for 20 min on ice, samples were centrifuged at 18,000*g* for 20 min, at 20 °C. An aliquot of each sample (50 μL) was diluted to a final volume of 250 μL in assay buffer consisting of 50 mM HEPES, 10% sucrose, 0.1% CHAPS, and 10 mM dithiothreitol supplemented with 100 μM of the colorimetric caspase-3, 8 or 9 substrates (*N*-acetyl-Asp-Glu-Val-Asp-*p*-nitroanilide, *N*-acetyl-Ile-Glu-Thr-Asp-*p*-nitroanilide and Ac-Leu-Glu-His-Asp-*p*-nitroanilide, respectively). Samples were incubated for 120 min at 37 °C and the absorbance was measured at 405 nm (Weinmann et al., 1999).

2.2.8. Statistical analysis

Statistics were calculated using GraphPad Prism™ (version 5.0; GraphPad Software). The results are expressed as the mean ± SEM (from at least four individual experiments). Statistical comparison between groups was performed using the one-way analysis of variance, followed by Bonferroni's post hoc test. The values of p lower than 0.05 were considered as statistically significant.

3. Results

3.1. Characterization of iron oxide nanoparticles

Both PAA-coated and non-coated ION particles have a similar size distribution, with a mean particle size of 9.9 ± 2.3 nm and 10.1 ± 2.4 nm (Mean ± SD) for the non-coated and PAA-coated ION, respectively (Figs. 1 and 2 of Appendices A and B). Although non-coated (without polymer) ION nanoparticles may be stable in water, they easily agglomerate by changing the pH (due to the change of the surface charge) or increasing the ionic strength (due to the shielding of surface charge). In fact, non-coated particles are only stable at basic pHs, and are already destabilized at pHs below ≈9 (surface charge ≈< −25 mV). However, PAA-coated particles are perfectly stable at neutral and even at slightly acid pHs (above ≈6)

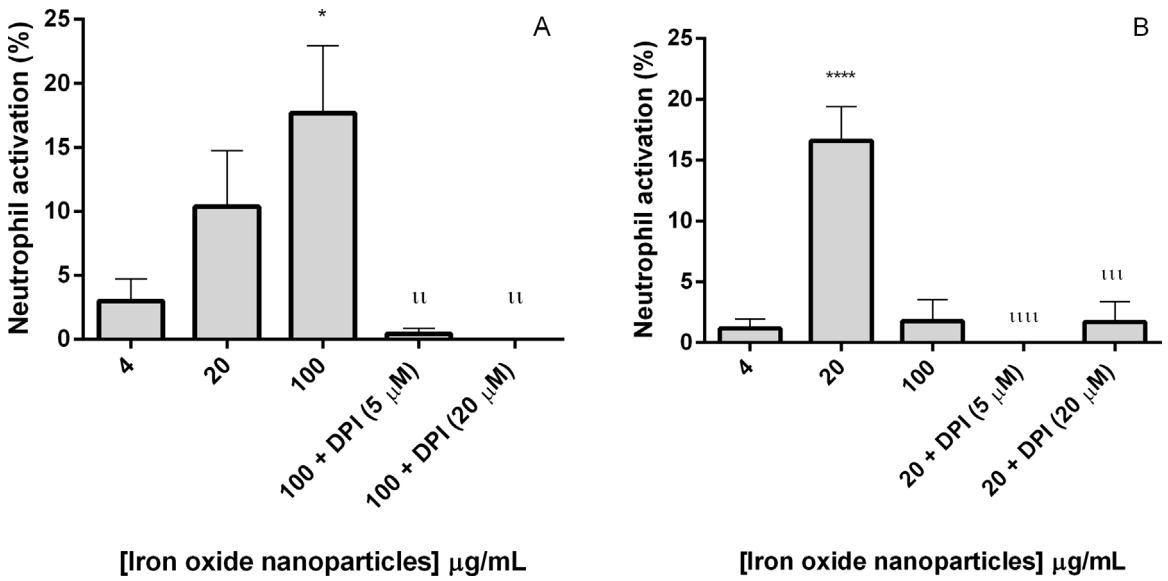

Fig. 1. Neutrophils' oxidative burst in cells exposed to (A) PAA-coated ION (4–100 μg/mL) and (B) non-coated ION (4–100 μg/mL) in the absence and presence of DPI, at 37 °C for 24 h. $^{*}p < 0.05$ and $^{****}p < 0.0001$ comparatively to control (without ION), $^{ιι}p < 0.01$ comparatively to 100 μg/mL PAA-coated ION and $^{ιιι}p < 0.001$ and $^{ιιιι}p < 0.0001$ comparatively to 20 μg/mL non-coated ION. Data are expressed as percentage of neutrophil activation. Values are given as mean ± SEM ($n \geq 4$).

(Fig. 3 of Appendices A and B). Concerning the stability is associated with the ionic strength, it was observed again that non-coated particles are destabilized already at NaCl concentrations ≈0.1 mM, while PAA-coated particles need ≈0.01 M to be destabilized (Fig. 4 of Appendices A and B). When the ION were dispersed in RPMI 1640 medium, the large hydrodynamic sizes observed and the fact that zeta potential was approximately 0 mV indicates that both types of nanoparticles tend to agglomerate when resuspended in this medium, though in much higher intensity in the case of non-coated ION (Fig. 5 of Appendices A and B).

3.2. Effect of ION on neutrophils' oxidative burst

Neutrophils' oxidative burst was assessed using the probe DHR (10 μM) in neutrophils exposed to PAA-coated and non-coated ION (4–100 μg/mL) and ION with DPI (20 μM) at 37 °C for 24 h (Fig. 1A and 1B). The neutrophils' oxidative burst was observed in the presence of both ION. This effect followed a concentration-dependent manner for PAA-coated nanoparticles, but in the case of non-coated ION, it occurred in a concentration-independent manner, having achieved the maximum activation at 20 μg/mL. The activation of oxidative burst triggered by both ION was approximately 20 times lower than positive control PMA (396 ± 49%). However, it was considered statistically significant, as it can be seen in Fig. 1A and B. Activation was blocked in the presence of DPI (20 μM), which means that the neutrophils' oxidative burst observed in the presence of both nanoparticles is due to NADPH oxidase activation.

3.3. Effect of ION on neutrophils' death by necrosis

No effect was found for any of the PAA-coated and non-coated ION (4–100 μg/mL) both at the trypan blue and LDH leakage assays (data not shown), which demonstrates that the ION studied do not seem to disrupt the cellular membrane at the present experimental conditions.

3.4. Effect of ION on neutrophils' death by apoptosis

3.4.1. Apoptosis evaluated by morphology

As it can be observed in 2A and B and 3B, the percentage of apoptotic cells increased in the presence of PAA-coated ION relatively to control (without ION), in a concentration-dependent manner.

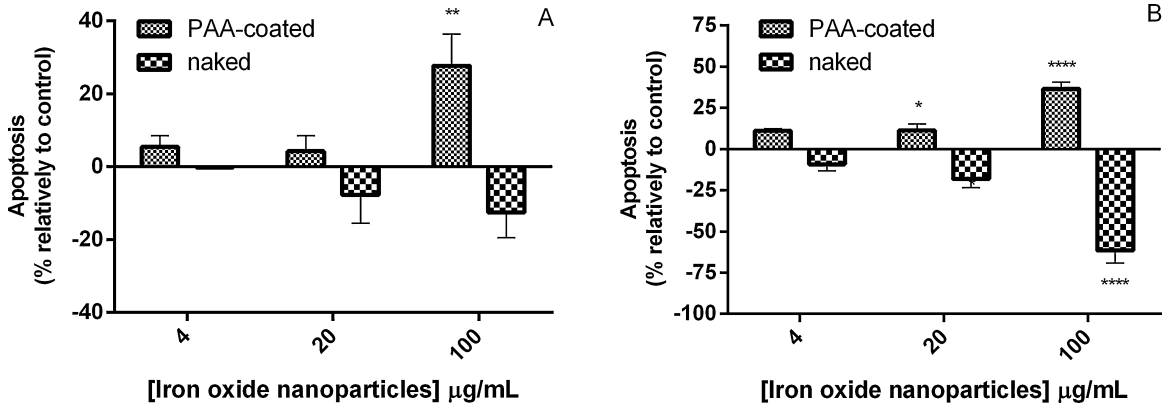

Fig. 2. Neutrophils' apoptosis assessed by microscopic morphology after exposure to PAA-coated and non-coated ION (4–100 μg/mL) at 37 °C: (A) 16 h and (B) 24 h. $^{*}p < 0.05$, $^{**}p < 0.01$ and $^{****}p < 0.0001$ comparatively to control (without ION). Data are expressed as percentage of apoptosis relatively to control. Values are given as mean ± SEM ($n \geq 4$).

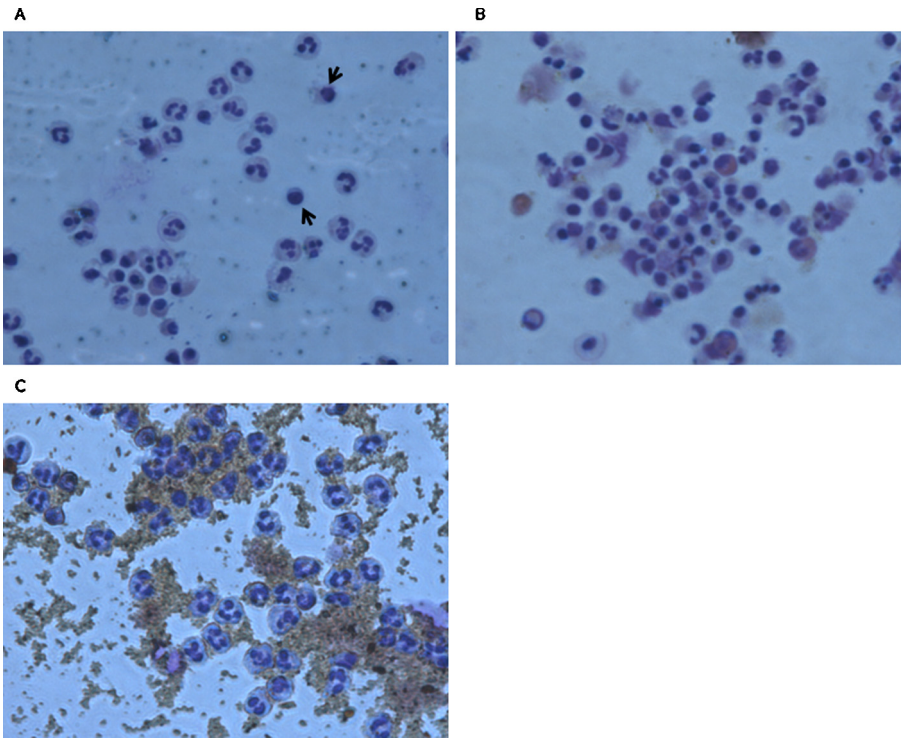

Fig. 3. Neutrophils' apoptosis assessed by microscopic morphology at 16 h: without ION (A), with 100 μg/mL PAA-coated ION (B) and 100 μg/mL non-coated ION (C) (amplification 40×). Arrowheads indicate apoptotic neutrophils.

On the contrary, the percentage of apoptotic cells decreased in the presence of non-coated ION (2A and B and 3C), which indicates that these nanoparticles exert the opposite effect of PAA-coated ION, having the capacity of protecting neutrophils from apoptosis.

3.4.2. Apoptosis evaluated by flow cytometry

It was verified that the proportion of annexin-V(+)/PI(−) cells increased in the presence of PAA-coated ION, in a concentration-dependent manner (4A and 5B). This demonstrates, once again, that PAA-coated ION cause acceleration of apoptotic death. On the contrary, the proportion of annexin-V(+)/PI(−) cells decreased in the presence of non-coated ION, in a concentration-dependent manner (4B and 5C). This result is in agreement with the previous results that demonstrate that this type of nanoparticles is able to protect neutrophils from apoptosis.

3.5. Apoptotic signalling

3.5.1. p53-DNA binding

Regarding PAA-coated ION, a marked heterogeneity was observed among subjects, evidencing two different groups of individuals' neutrophils: one of the groups (non-responders) did not present any increase in p53 activity in the presence of the nanoparticles, when compared to the control; the other group (responders) presented a significant increase in p53 activity in the presence of these nanoparticles, well evidenced for the concentrations of 20

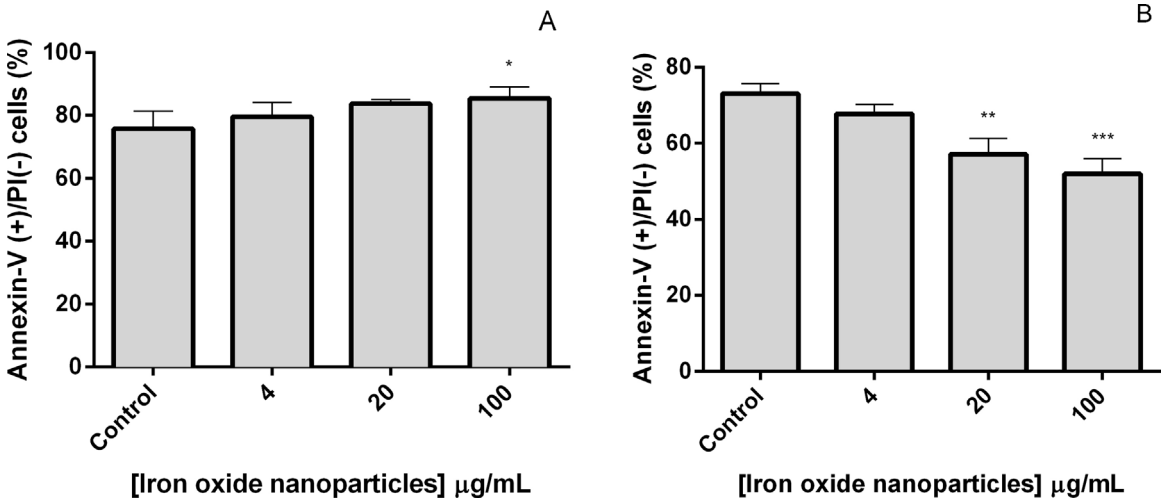

Fig. 4. Neutrophils' apoptosis assessed by flow cytometry after exposure to (A) PAA-coated ION (4–100 μg/mL) and (B) non-coated ION (4–100 μg/mL) at 37 °C for 16 h. $^{*}p < 0.05$, $^{**}p < 0.01$ and $^{***}p < 0.001$ comparatively to control. Data are expressed as percentage of annexin-V(+)/PI(−) cells. Values are given as mean ± SEM ($n \geq 4$).

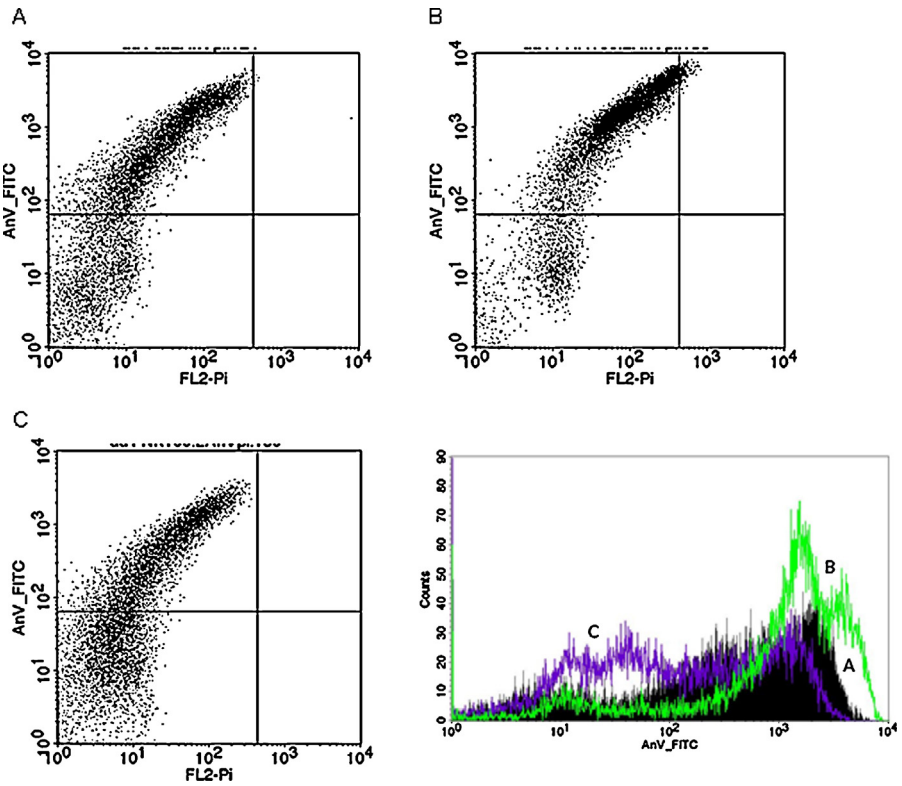

Fig. 5. Flow cytometric analysis of annexin V binding assay. Neutrophils incubated at 37 °C for 16 h without ION (A—black area) and with 100 μg/mL PAA-coated (B—green curve) and non-coated (C—blue curve) ION. (For interpretation of the references to color in this figure legend, the reader is referred to the web version of this article.)

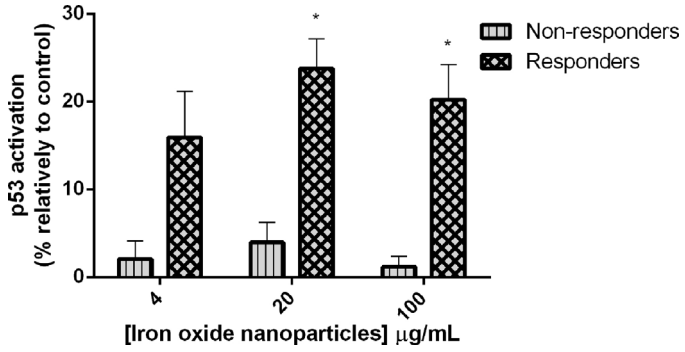

Fig. 6. p53 activation in neutrophils exposed to PAA-coated ION (4–100 μg/mL) at 37 °C for 24 h. *$p < 0.05$ comparatively to control (without ION). Data are expressed as percentage of p53 activation relatively to control. Values are given as mean ± SEM ($n \geq 4$).

and 100 μg/mL (Fig. 6). Non-coated ION did not influence p53 activity (data not shown).

3.5.2. *Measurement of caspases 3, 8 and 9 activities*

Concerning PAA-coated ION, it was observed that caspases 3, 8 and 9 activities were increased in the presence of ION, in a concentration-dependent manner (7A and B, 8A and 9A and B). For the non-coated ION, the opposite effect was observed for caspases 3 and 9, given that these nanoparticles exhibited the ability to inhibit caspases 3 and 9 activity, comparatively to control (without ION) (7A and B and 9A and B). However, they did not alter the caspase 8 activity comparatively to control (data not shown). These results are in agreement with those obtained in the evaluation of apoptosis.

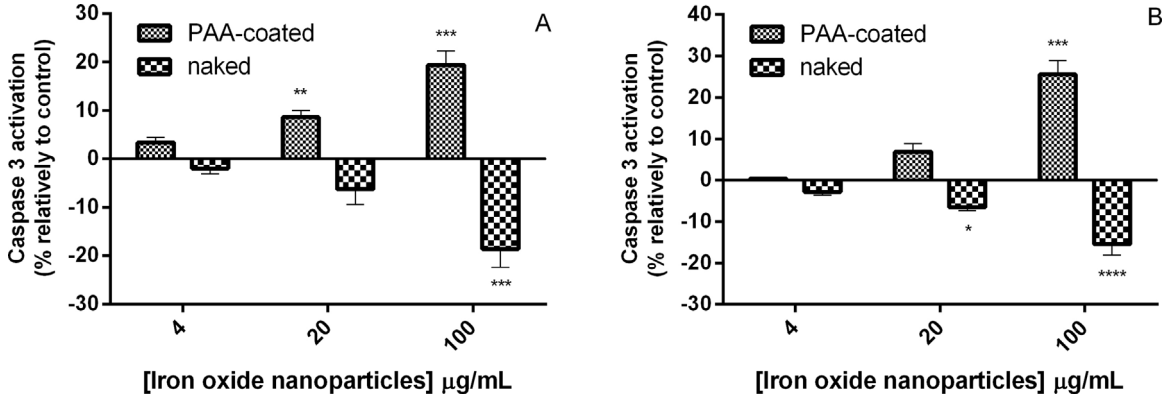

Fig. 7. Caspase 3 activity in neutrophils exposed to PAA-coated and non-coated ION (4–100 μg/mL) at 37 °C: (A) 16 h and (B) 24 h. *$p < 0.05$, **$p < 0.01$, ***$p < 0.001$ comparatively to control (without ION). Data are expressed as percentage of caspase 3 activation relatively to control. Values are given as mean ± SEM ($n \geq 4$).

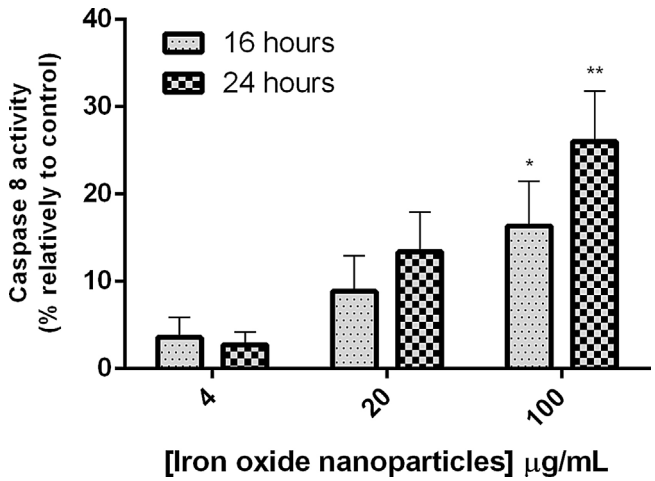

Fig. 8. Caspase 8 activity in neutrophils exposed to PAA-coated ION (4–100 μg/mL) at 37 °C for 16 and 24 h. $^{*}p < 0.05$ and $^{**}p < 0.01$ comparatively to control. Data are expressed as percentage of caspase 8 activation relatively to control (without ION). Values are given as mean ± SEM ($n \geq 4$).

4. Discussion

This work was undertaken to evaluate the putative capacity of PAA-coated and non-coated ION to activate the oxidative burst in human neutrophils and to modify their lifespan *in vitro*. It was clearly evidenced that both ION studied were able to trigger neutrophils' oxidative burst and that PAA-coated ION increased, while non-coated ION decreased, apoptotic signaling and apoptosis.

Neutrophil's oxidative burst occurred in a concentration-dependent manner following exposure to PAA-coated ION. For non-coated ION, the highest neutrophil activation was observed for 20 μg/mL, probably due to NADPH oxidase inhibition at the higher concentration tested (100 μg/mL). In both cases, the observed oxidative burst was reverted in the presence of a NADPH oxidase inhibitor (DPI), which demonstrates the full involvement of NADPH oxidase activation in the observed effect. This enzyme reduces molecular oxygen to superoxide radical $\left(O_2^{-}\cdot\right)$ in the presence of NADPH. After $O_2^{-}\cdot$ production, other ROS, namely hydrogen peroxide (H_2O_2), hypochlorous acid (HOCl), hydroxyl radical ($HO^{\bullet}$) and singlet oxygen ($^1O_2$), and RNS, particularly nitric oxide ($^{\bullet}NO$) and peroxynitrite anion ($ONOO^{-}$), are formed in cascade (Brasen et al., 2010; Freitas et al., 2009a,b), which characterizes the neutrophils' oxidative burst. Although the interaction of PAA-coated ION with neutrophils is reported for the first time in the present study, ION with other types of coatings have been shown to promote ROS production in other cell types. Bae et al. (2011), using 2′,7′-dichlorofluorescein diacetate (DCFH-DA), demonstrated that carboxydextran-coated ION increased intracellular levels of ROS in mouse hepatocytes, and Lunov et al. (2010a,b) demonstrated that carboxydextran-coated superparamagnetic ION induced a time-dependent ROS production in human macrophages. Choi et al. (2009) also showed that anionic clay layered ION caused an increase in ROS production in human lung cancer A549 cells. On the other hand, Karlsson et al. (2008) observed, also using DCFH-DA, that non-coated ION do not potentiate the ROS production in A549 type II lung epithelial cells. Since the concentrations tested were similar in these different studies, it is important to highlight that the ION effects can be distinct according to the type of coating, or the type of cells tested. While neutrophils, monocytes and macrophages may react to ION through the activation of NADPH oxidase, as shown in the present study for neutrophils, other mechanisms may also be involved in the production of ROS. Shubayev et al. (2009) hypothesized that ION induce redox cycling and catalytic chemistry *via* Fenton reaction. Our study did not ascertain the intervention of ION in this reaction. Nevertheless, once NADPH oxidase is activated, the cascade of ROS and RNS production succeeds, and $HO^{\bullet}$ is expected to be generated through the Fenton reaction.

The formation of ROS and RNS, and ensuing oxidative stress may intervene in apoptotic pathways, namely through the activation of the mitochondrial apoptotic pathway (Franco et al., 2009). In fact, there are reports concerning the ability of ROS and RNS to interfere directly in apoptosis through mitochondrial membrane permeabilization and cytochrome c release, as well as in Jun N-terminal protein kinase (JNK) activation (Circu and Aw, 2010; Huang et al., 2008). Another pathway involving ROS and RNS is through direct activation of p53 (Sharma et al., 2012). It is thought that ROS and RNS-induced DNA damage may trigger p53 activation (Simbula et al., 2007). Phosphorylation in response to DNA damage enhances the interaction of p300 and PCAF with p53, thereby leading to p53 acetylation and consequent activation (Sakaguchi et al., 1998). Therefore, these two pathways may be connected to each other. In fact, the activation of p53 triggers the expression of Bax and Noxa, two pro-apoptotic proteins that induce an increase in mitochondrial permeability, leading to the release of cytochrome c, apoptosis inducing factor (AIF) and Diablo/Smac and the consequent mitochondrial apoptotic pathway (Chen and Shi, 2002). Besides the above rationale, the expression of pro-apoptotic proteins and/or the decrease in anti-apoptotic proteins may be activated by several other factors and/or stimuli. For example, Miyake et al. (2012) stated that rapamycin induces p53-independent mitochondrial apoptosis by decreasing anti-apoptotic proteins.

In the present study, p53 activation by PAA-coated ION was demonstrated, for the first time, in part of the subjects tested. In line

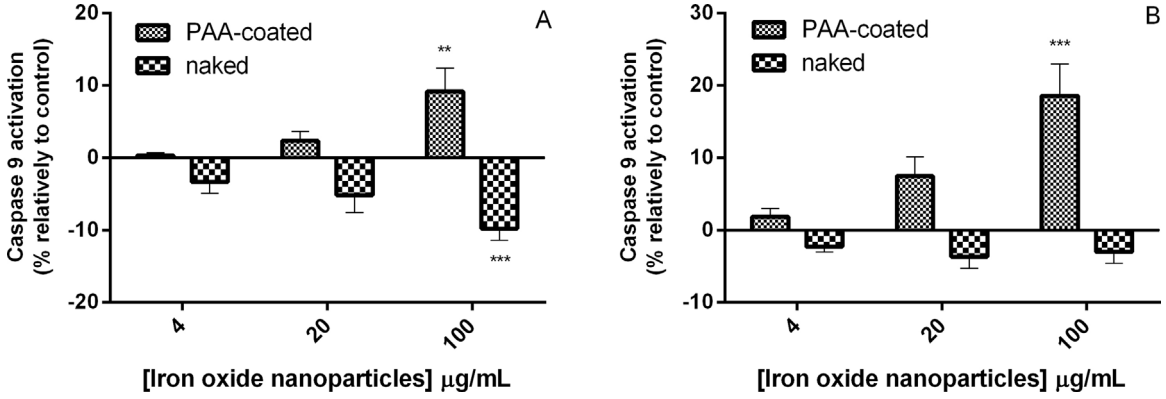

Fig. 9. Caspase 9 activity in neutrophils exposed to PAA-coated and non-coated ION (4–100 μg/mL) at 37 °C: (A) 16 h and (B) 24 h. $^{**}p < 0.01$ and $^{***}p < 0.001$ comparatively to control (without ION). Data are expressed as percentage of caspase 9 activation relatively to control. Values are given as mean ± SEM ($n \geq 4$).

with these results, Wu et al. (2012) and Wu and Sun (2011) have reported before that non-coated ION induced p53 gene expression and increased phosphorylation levels of p53 in PC12 cells, and that this activation is associated with increased levels of Bax and decreased levels of Bcl-2. On the other hand, the opposite was also reported by Huang et al. (2009), in which it was referred slight decreases in p53 expression in ferucarbotran-labeled human mesenchymal stem cells, and it was also reported that ION do not change the expression of p53 mRNA in K562/A02 cells (Chen et al., 2009). While this activation may represent a link, as described above, between ROS and an apoptotic pathway, the truth is that p53 did not demonstrate to be essential for neutrophil activation in our study, given that apoptosis activation occurred for all donors tested with PAA-coated ION, while p53 activation occurred only for one group (named responders).

In this study, the proportion of apoptotic cells was increased in the presence of PAA-coated ION, in a concentration-dependent manner. However, the results obtained with these ION seem to be more evident for the morphologic assay, comparatively to the flow cytometry assay. This happens because, when cells are annexin V+, this means that phosphatidylserine was translocated to the outer cell membrane leaflet, an event that occurs during apoptotic process (Lunov et al., 2010a,b). Thus, it is possible that some of the cells have already initiated the process of apoptosis, even in control, although they do not present the characteristic apoptotic morphology when they are counted on the morphologic assay, presenting already the phosphatidylserine on the outer side of the membrane leaflet. Therefore, annexin V+ control cells is approximately 80% and, consequently, the increase after treatment with PAA-coated ION will not be so evident as it is in cytospin assay. Nevertheless, it is evident that these ION have the ability to accelerate a natural feature of neutrophils that correspond to a short lifespan mediated by apoptosis. In contrast, in the presence of non-coated ION, the proportion of apoptotic cells decreased in a concentration-dependent manner. Likewise, Lunov et al. (2010a,b) reported that exposure of macrophages to carboxydextran-coated superparamagnetic ION triggered translocation of phosphatidylserine to the outer cell membrane leaflet, indicating increased apoptosis. Choi et al. (2009) also reported that non-coated ION triggered the same in human lung cancer A549 cells. On the other hand, it was previously reported a lack of effect of non-coated ION on mature mouse dendritic cells' apoptosis (Mou et al., 2011). Once again, it is important to highlight that the effect of ION is not necessarily the same in different types of cells, namely in what concerns to the production of reactive species and ensuing apoptotic signaling.

For a better clarification of the apoptotic pathways involved in the observed pro- and anti-apoptotic effects, caspases 3, 8 and 9 activities were assessed. It was observed that the activities of caspases 3, 8 and 9 were increased in the presence of PAA-coated ION, in a concentration-dependent manner. Given that caspase 8 is involved in the extrinsic apoptotic pathway and caspase 9 is involved in the mitochondrial apoptotic pathway (Chen and Shi, 2002; Franco et al., 2009; Letuve et al., 2002), these data suggest that PAA-coated ION interfere with both apoptotic pathways, promoting the apoptosis acceleration by both pathways. Regarding caspase 3, as this is one of the effector caspases, intervening in a late apoptosis stage, common to mitochondrial and extrinsic pathways, its increase just corroborates the activation of signaling caspases. Caspase 3 activity increase was previously shown to be triggered by carboxydextran-coated ION in a mouse liver cell line (NCTC 1469) (Bae et al., 2011). Likewise, Lunov et al. (2010a,b) reported that carboxydextran-coated superparamagnetic ION and ultrasmall superparamagnetic ION increased the caspase 3 activity in human macrophages. Dilnawaz et al. (2012) also reported an increase in caspases 3 and 9 activation caused by transferring-conjugated curcumin-loaded superparamagnetic ION in the leukemic cell line K562. It was also found by Zhang et al. (2011) that tetraheptylammonium-coated ION have the capacity to increase the ability of daunorubucin to induce apoptosis in K562 cells through caspase 8 activation, which is in accordance to our results. These results suggest that coating may be important for the activation of apoptotic signaling, by maintaining ION dispersed, though the type of coating may not have an important role in the final effect, though this assumption needs further evaluation. For non-coated ION, it was observed that these nanoparticles exhibit the capacity to inhibit caspases 3 and 9 activation, explaining why these nanoparticles induce a delay in the apoptotic process. These results are in accordance with Khan et al. (2011), which showed that non-coated ION reduced caspase 9 activity in HeLa cells. The fact that non-coated ION inhibited caspases 3 and 9 but did not interfere with caspase 8 demonstrates that these nanoparticles only inhibited the mitochondrial apoptotic pathway, not interfering with the extrinsic apoptotic pathway. Although, at the present stage, the mechanism(s) involved could not be determined, this is an important finding to be considered upon exposure to ION in the workplace and in the environment.

This study also shows that none of the studied ION studied seem to alter neutrophils' lifespan by necrosis. These results are in agreement with the studies of Karlsson et al. (2008), which demonstrated that non-coated ION did not influence cellular necrosis in cultured A549 type II lung epithelial cells. Furthermore, Wang et al. (2009) performed a study in order to assess the dextran-coated ION effect on rat adipose-derived stem cells, reaching the same conclusions. Hussain et al. (2005) used the LDH leakage methodology and stated that the non-coated ION do not produce cytotoxicity up to the concentration of 100 μg/mL in BRL 3A RAT liver cells. However, for similar concentrations, Choi et al. (2009) reported that non-coated ION cause an increase in LDH leakage in human lung cancer A549 cells, which means that these nanoparticles can have different toxicologic mechanisms, according to the cells they are in contact with.

Concerning the limitations of the present study, the fact that it was performed *in vitro* does not consider the interaction existing between different cells that occur *in vivo*. Therefore, the factors produced by adjacent cells that occur *in vivo* and may influence the mode how different physiological processes occur, namely apoptosis and neutrophil activation, are not taken into account in this study. Another factor that cannot be studied *in vitro* is the bone marrow and macrophage response to a smaller neutrophils' lifespan, and therefore how a new equilibrium may be reached *in vivo*. The concentrations used in our study do not seem to constitute a limitation, since they are in accordance with the ones used in therapeutic applications: for magnetic resonance imaging, the concentration usually used is around 45 μmol Fe/kg, which is about the concentration of 70 μg/mL (for 50 kg human weight and 5000 mL human blood volume) (Apopa et al., 2009).

5. Conclusion

In this study it was evaluated the ability of PAA-coated and non-coated ION to induce oxidative burst in human neutrophils and to influence the respective death trends. The obtained results show that both ION induce oxidative burst through NAPDH-oxidase activation. It was also shown that, while necrosis was not affected, PAA-coated ION accelerate the apoptotic death of human neutrophils by the mitochondrial and extrinsic pathways. p53 revealed not to be essential to this effect. However, for some donors, PAA-coated ION showed to be able to activate p53. Non-coated ION showed to inhibit the mitochondrial pathway, not interfering with the extrinsic pathway.

Though these effects still need to be confirmed *in vivo*, the observed effects may have important clinical implications in the

event of their use for the improvement of site-specific drug or gene delivery, in magnetic resonance imaging contrast, hyperthermia treatments in cancer therapy, magnetofection, and stem cell therapy.

Conflict of interest statement

None declared.

Acknowledgments

Authors declare no conflicts of interest concerning the present study. Diana Couto and Vânia Vilas-Boas acknowledge the FCT financial support for the Ph.D. grants (SFRH/BD/72856/2010 and SFRH/BD/82556/2011, respectively) and Marisa Freitas for her Pos-doc grant (SFRH/BPD/76909/2011), in the ambit of "POPH–QREN—Tipologia 4.1—Formação Avançada" co-sponsored by FSE and national funds of MCTES. The authors greatly acknowledge the financial support given by Reitoria da Universidade do Porto and Santander Totta for Projectos IJUP 2011.

Appendix A. Supplementary data

Supplementary data associated with this article can be found, in the online version, at http://dx.doi.org/10.1016/j.toxlet.2013.11.020.

References

Apopa, P.L., et al., 2009. Iron oxide nanoparticles induce human microvascular endothelial cell permeability through reactive oxygen species production and microtubule remodeling. Part. Fibre Toxicol. 6, 1.
Bae, J.E., et al., 2011. The effect of static magnetic fields on the aggregation and cytotoxicity of magnetic nanoparticles. Biomaterials 32 (35), 9401–9414.
Bockmann, S., et al., 2001. Delay of neutrophil apoptosis by the neuropeptide substance P: involvement of caspase cascade. Peptides 22 (4), 661–670.
Brasen, J.C., et al., 2010. On the mechanism of oscillations in neutrophils. Biophys. Chem. 148 (1-3), 82–92.
Chen, B., et al., 2009. Magnetic nanoparticle of Fe_3O_4 and 5-bromotetrandrin interact synergistically to induce apoptosis by daunorubicin in leukemia cells. Int. J. Nanomed. 4, 65–71.
Chen, F., Shi, X., 2002. Intracellular signal transduction of cells in response to carcinogenic metals. Crit. Rev. Oncol. Hematol. 42 (1), 105–121.
Choi, S.J., et al., 2009. Toxicological effects of inorganic nanoparticles on human lung cancer A549 cells. J. Inorg. Biochem. 103 (3), 463–471.
Circu, M.L., Aw, T.Y., 2010. Reactive oxygen species, cellular redox systems, and apoptosis. Free Radical Biol. Med. 48 (6), 749–762.
Dilnawaz, F., et al., 2012. Transferrin-conjugated curcumin-loaded superparamagnetic iron oxide nanoparticles induce augmented cellular uptake and apoptosis in K562 cells. Acta Biomater. 8 (2), 704–719.
Fadeel, B., et al., 1998. Involvement of caspases in neutrophil apoptosis: regulation by reactive oxygen species. Blood 92 (12), 4808–4818.
Franco, R., et al., 2009. Environmental toxicity, oxidative stress and apoptosis: menage a trois. Mutat. Res. Genet. Toxicol. Environ. Mutagen. 674 (1-2), 3–22.
Freitas, M., et al., 2013a. Nickel induces apoptosis in human neutrophils. Biometals 26 (1), 13–21.
Freitas, M., et al., 2013b. Acetaminophen prevents oxidative burst and delays apoptosis in human neutrophils. Toxicol. Lett. 219 (2), 170–177.
Freitas, M., et al., 2010. Nickel induces oxidative burst, NF-kappaB activation and interleukin-8 production in human neutrophils. J. Biol. Inorg. Chem. 15 (8), 1275–1283.
Freitas, M., et al., 2009a. Optical probes for detection and quantification of neutrophils' oxidative burst: a review. Anal. Chim. Acta 649 (1), 8–23.
Freitas, M., et al., 2008. Isolation and activation of human neutrophils in vitro. The importance of the anticoagulant used during blood collection. Clin. Biochem. 41 (7–8), 570–575.
Freitas, M., et al., 2009b. Optimization of experimental settings for the analysis of human neutrophils oxidative burst in vitro. Talanta 78 (4–5), 1476–1483.
Goncalves, D.M., et al., 2010. Activation of human neutrophils by titanium dioxide (TiO_2) nanoparticles. Toxicol. In Vitro 24 (3), 1002–1008.
Hong, S.C., et al., 2011. Subtle cytotoxicity and genotoxicity differences in superparamagnetic iron oxide nanoparticles coated with various functional groups. Int. J. Nanomed. 6, 3219–3231.
Huang, D.M., et al., 2009. The promotion of human mesenchymal stem cell proliferation by superparamagnetic iron oxide nanoparticles. Biomaterials 30 (22), 3645–3651.
Huang, J., et al., 2008. Reactive oxygen species mediate oridonin-induced HepG2 apoptosis through p53, MAPK, and mitochondrial signaling pathways. J. Pharmacol. Sci. 107 (4), 370–379.
Hussain, S.M., et al., 2005. In vitro toxicity of nanoparticles in BRL 3A rat liver cells. Toxicol. In Vitro 19 (7), 975–983.
Karlsson, H.L., et al., 2008. Copper oxide nanoparticles are highly toxic: a comparison between metal oxide nanoparticles and carbon nanotubes. Chem. Res. Toxicol. 21 (9), 1726–1732.
Khan, J.A., et al., 2011. Magnetite (Fe_3O_4) nanocrystals affect the expression of genes involved in the TGF-beta signalling pathway. Mol.Biosyst. 7 (5), 1481–1486.
Kroemer, G., et al., 2007. Mitochondrial membrane permeabilization in cell death. Physiol. Rev. 87 (1), 99–163.
Letuve, S., et al., 2002. Critical role of mitochondria, but not caspases, during glucocorticosteroid-induced human eosinophil apoptosis. Am. J. Respir. Cell Mol. Biol. 26 (5), 565–571.
Lunov, O., et al., 2010a. The effect of carboxydextran-coated superparamagnetic iron oxide nanoparticles on c-Jun N-terminal kinase-mediated apoptosis in human macrophages. Biomaterials 31 (19), 5063–5071.
Lunov, O., et al., 2010b. Lysosomal degradation of the carboxydextran shell of coated superparamagnetic iron oxide nanoparticles and the fate of professional phagocytes. Biomaterials 31 (34), 9015–9022.
Massart, R., et al., 1995. Preparation and properties of monodisperse magnetic fluids. J. Magn. Magn. Mater. 149 (1-2), 1–5.
Matsushita, T., et al., 2011. Inflammatory imaging with ultrasmall superparamagnetic iron oxide. Magn. Reson. Imaging 29 (2), 173–178.
Miyake, N., et al., 2012. Rapamycin induces p53-independent apoptosis through the mitochondrial pathway in non-small cell lung cancer cells. Oncol. Rep. 28 (3), 848–854.
Mou, Y., et al., 2011. Influence of synthetic superparamagnetic iron oxide on dendritic cells. Int. J. Nanomed. 6, 1779–1786.
Muller, K., et al., 2007. Effect of ultrasmall superparamagnetic iron oxide nanoparticles (Ferumoxtran-10) on human monocyte-macrophages in vitro. Biomaterials 28 (9), 1629–1642.
Naqvi, S., et al., 2010. Concentration-dependent toxicity of iron oxide nanoparticles mediated by increased oxidative stress. Int. J. Nanomed. 5, 983–989.
Pineiro-Redondo, Y., et al., 2011. The influence of colloidal parameters on the specific power absorption of PAA-coated magnetite nanoparticles. Nanoscale Res. Lett. 6 (1), 383.
Roohi, F., et al., 2012. Studying the effect of particle size and coating type on the blood kinetics of superparamagnetic iron oxide nanoparticles. Int. J. Nanomed. 7, 4447–4458.
Rowe, S.J., et al., 2002. Caspase-1-deficient mice have delayed neutrophil apoptosis and a prolonged inflammatory response to lipopolysaccharide-induced acute lung injury. J. Immunol. 169 (11), 6401–6407.
Sakaguchi, K., et al., 1998. DNA damage activates p53 through a phosphorylation-acetylation cascade. Genes Dev. 12 (18), 2831–2841.
Saldanha-Gama, R.F., et al., 2010. Alpha(9)beta(1) integrin engagement inhibits neutrophil spontaneous apoptosis: involvement of Bcl-2 family members. Biochim. Biophys. Acta, Mol. Cell Res. 1803 (7), 848–857.
Sharma, V., et al., 2012. Zinc oxide nanoparticles induce oxidative DNA damage and ROS-triggered mitochondria mediated apoptosis in human liver cells (HepG2). Apoptosis 17 (8), 852–870.
Shubayev, V.I., et al., 2009. Magnetic nanoparticles for theragnostics. Adv. Drug Deliv. Rev. 61 (6), 467–477.
Simbula, G., et al., 2007. Increased ROS generation and p53 activation in alpha-lipoic acid-induced apoptosis of hepatoma cells. Apoptosis 12 (1), 113–123.
Sladek, Z., et al., 2005. Neutrophil apoptosis during experimentally induced Staphylococcus aureus mastitis. Vet. Res. 36 (4), 629–643.
Thompson, T., et al., 2004. Phosphorylation of p53 on key serines is dispensable for transcriptional activation and apoptosis. J. Biol. Chem. 279 (51), 53015–53022.
Turina, M., et al., 2005. Endotoxin inhibits apoptosis but induces primary necrosis in neutrophils. Inflammation 29 (1), 55–63.
Wang, L., et al., 2009. Superparamagnetic iron oxide does not affect the viability and function of adipose-derived stem cells, and superparamagnetic iron oxide-enhanced magnetic resonance imaging identifies viable cells. Magn. Reson. Imaging 27 (1), 108–119.
Watson, R.W., et al., 1998. The IL-1 beta-converting enzyme (caspase-1) inhibits apoptosis of inflammatory neutrophils through activation of IL-1 beta. J. Immunol. 161 (2), 957–962.
Weinmann, P., et al., 1999. Bcl-Xl- and Bax-alpha-mediated regulation of apoptosis of human neutrophils via caspase-3. Blood 93 (9), 3106–3115.
Wu, J., et al., 2012. Neurotoxic potential of iron oxide nanoparticles in the rat brain striatum and hippocampus. Neurotoxicology 34, 243–253.
Wu, J., Sun, J., 2011. Investigation on mechanism of growth arrest induced by iron oxide nanoparticles in PC12 cells. J. Nanosci. Nanotechnol. 11 (12), 11079–11083.
Zhang, G., et al., 2011. Fe_3O_4 nanoparticles with daunorubicin induce apoptosis through caspase 8-PARP pathway and inhibit K562 leukemia cell-induced tumor growth in vivo. Nanomedicine 7 (5), 595–603.
Zhu, M.T., et al., 2011. Endothelial dysfunction and inflammation induced by iron oxide nanoparticle exposure: risk factors for early atherosclerosis. Toxicol. Lett. 203 (2), 162–171.